

LETTER TO THE EDITOR

The metal–insulator transition and ferromagnetism in the electron-doped layered manganites $\text{La}_{2.3-x}\text{Y}_x\text{Ca}_{0.7}\text{Mn}_2\text{O}_7$ ($x = 0, 0.3, 0.5$)

P Raychaudhuri†, C Mitra, A Paramekanti, R Pinto, A K Nigam and S K Dhar

Tata Institute of Fundamental Research, Homi Bhaba Road, Colaba, Mumbai-400005, India

Received 13 November 1997, in final form 21 January 1998

Abstract. Bulk samples of $\text{La}_{2.3-x}\text{Y}_x\text{Ca}_{0.7}\text{Mn}_2\text{O}_7$, with $x = 0, 0.3, 0.5$, with layered perovskite structure have been synthesized and investigated as regards their electrical, electronic and magnetic properties. It is found that $\text{La}_{1.8}\text{Y}_{0.5}\text{Ca}_{0.7}\text{Mn}_2\text{O}_7$ has tetragonal structure and is a metallic ferromagnet with a magnetic transition temperature of 170 K. This compound shows metallic behaviour below 140 K and has a large magnetoresistance (MR) $|\Delta\rho/\rho_0| \sim 94\%$ at 100 K at 34 kOe. For $x = 0$ and 0.3 the structure is monoclinic with a suppression of metallicity. For $x = 0$ the material is a ferromagnetic insulator. We observed a large increase in the coefficient of the linear term in the specific heat with decreasing x . As far as we are aware, this is the first report of an electron-doped manganite showing a metal–insulator transition and ferromagnetism.

Hole-doped rare-earth manganese oxides have attracted considerable attention in recent times because of their magnetotransport phenomena arising from spin–charge coupling. Hole doping is achieved by partially replacing the trivalent rare-earth ion by a bivalent ion like Sr, Ca or Ba as a result of which the manganese ion goes into a $\text{Mn}^{3+}/\text{Mn}^{4+}$ mixed-valence state. Materials with the form $\text{R}_{1-x}\text{M}_x\text{MnO}_3$ (R is a rare-earth ion whereas M is a bivalent cation) with three-dimensional Mn–O–Mn bonds like those in $\text{La}_{1-x}\text{Ca}_x\text{MnO}_3$ and $\text{La}_{1-x}\text{Sr}_x\text{MnO}_3$ have been known for a long time to be paramagnetic insulators at high temperatures and ferromagnetic metals at low temperatures (for $x > 0.2$). In contrast, $\text{R}_{2-2x}\text{M}_{1+2x}\text{Mn}_2\text{O}_7$ compounds with layered perovskite structure have two-dimensional Mn–O–Mn networks in the a – b plane. Studies on $\text{La}_{2-2x}\text{Sr}_{1+2x}\text{Mn}_2\text{O}_7$ have shown that these materials show strong anisotropy between the a – b plane (in the plane) and along the c -axis (out of the plane) [1]. Ferromagnetism and a metal–insulator transition in this class of compounds were reported earlier for hole-doped $\text{La}_{2-2x}\text{Sr}_{1+2x}\text{Mn}_2\text{O}_7$ [1, 2] and $\text{La}_{2-2x}\text{Ca}_{1+2x}\text{Mn}_2\text{O}_7$ ($x > 0.4$) [3]. For $\text{Sr}_{2-x}\text{Nd}_{1+x}\text{Mn}_2\text{O}_7$ [4] the resistivity shows a complex behaviour but the material does not show any ferromagnetic transition. In all of these compounds the magnetic and electrical properties are governed by a Zener double-exchange mechanism based on the $\text{Mn}^{3+}/\text{Mn}^{4+}$ mixed-valence states [5].

In this letter we report on the magnetic, transport and electronic properties of the electron-doped manganites $\text{La}_{2.3-x}\text{Y}_x\text{Ca}_{0.7}\text{Mn}_2\text{O}_7$ ($x = 0, 0.3, 0.5$). Unlike the case for the compounds reported on earlier, here the R/M ratio is such that manganese goes into

† E-mail: pratap@tifrc3.tifr.res.in.

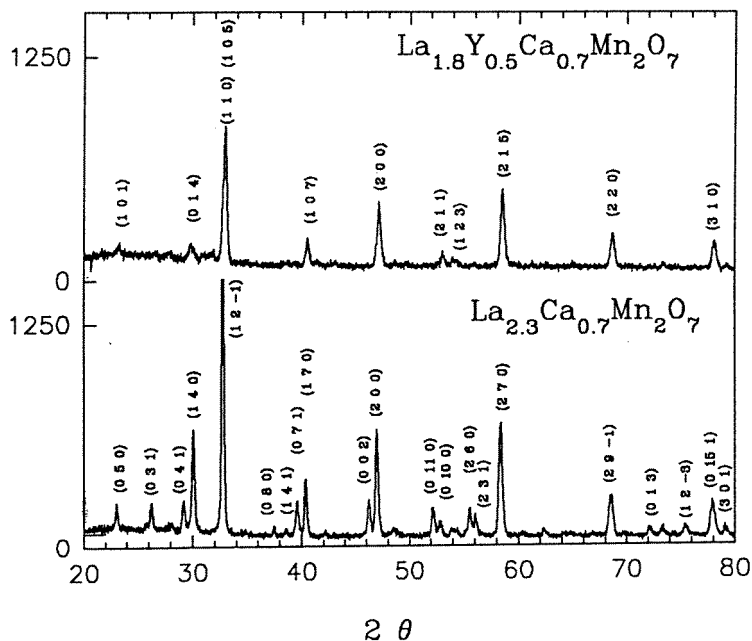


Figure 1. X-ray diffraction patterns of $\text{La}_{2.3-x}\text{Y}_x\text{Ca}_{0.7}\text{Mn}_2\text{O}_7$ samples with $x = 0, 0.05, 0.5$.

a $\text{Mn}^{2+}/\text{Mn}^{3+}$ mixed-valence state. The double exchange operates here in the $\text{Mn}^{2+}\text{-O-Mn}^{3+}$ bonds giving rise to ferromagnetism and a metal-insulator transition. The compound with $x = 0.5$ is a metal below 140 K and has a ferromagnetic transition temperature of 170 K. The material shows large negative magnetoresistance ($|\Delta\rho/\rho_0| \sim 94\%$ at 3.8 T at 100 K).

Bulk ceramic samples were prepared through the conventional solid-state reaction route starting from La_2O_3 , Y_2O_3 , CaCO_3 and MnO_2 . Stoichiometric amounts of the starting oxides and carbonates were mixed, ground and calcined in air for 18 h at 900 °C. The reacted powder was then reground, pelletized, sintered for 15 h at 1450 °C in flowing oxygen, cooled down to 1050 °C at 10 °C min^{-1} , kept for 10 h in flowing oxygen, and cooled to room temperature at 10 °C min^{-1} . The samples were characterized through x-ray diffraction (XRD) and energy-dispersive x-ray microanalysis (EDX), and using a scanning electron microscope (SEM). The cell constants were calculated using the XLAT software for the tetragonal structure. The composition was found to be nearly identical to the starting composition within the accuracy of 3% of EDX. The electrical resistance and magnetoresistance were measured using the conventional four-probe technique. The magnetoresistance (MR) was defined as $\Delta\rho/\rho_0 = (\rho(H = 0) - \rho(H))/\rho(H = 0)$. The magnetization was measured either using a Quantum Design SQUID magnetometer or by the Faraday method. The specific heat of these samples was measured using a home-made, semi-adiabatic, heat-pulse-type set-up calibrated with a copper standard with an accuracy of 4%.

Figure 1 shows representative XRD patterns of $\text{La}_{2.3-x}\text{Y}_x\text{Ca}_{0.7}\text{Mn}_2\text{O}_7$ ($x = 0$ and 0.5). All of the peaks for the composition $x = 0.5$ are indexed with respect to the tetragonal structure with lattice constants $a = 3.874$ Å and $c = 19.218$ Å. For $x = 0$ and 0.3 the

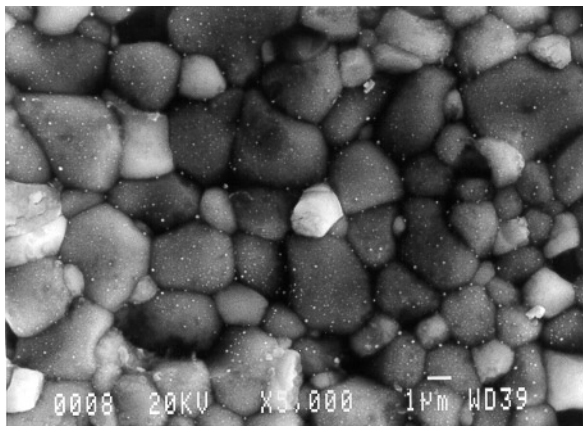


Figure 2. A SEM photograph of the $\text{La}_{1.8}\text{Y}_{0.5}\text{Ca}_{0.7}\text{Mn}_2\text{O}_7$ sample showing grains and grain boundaries.

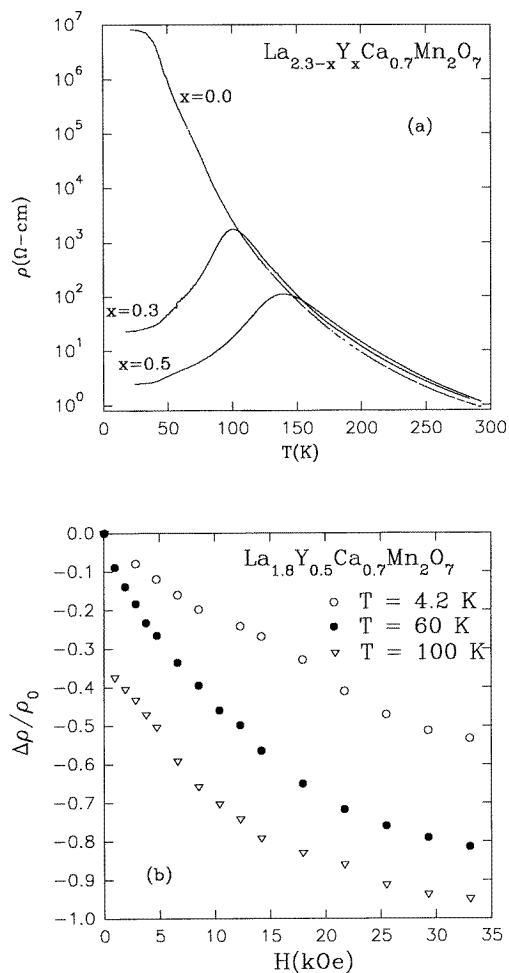
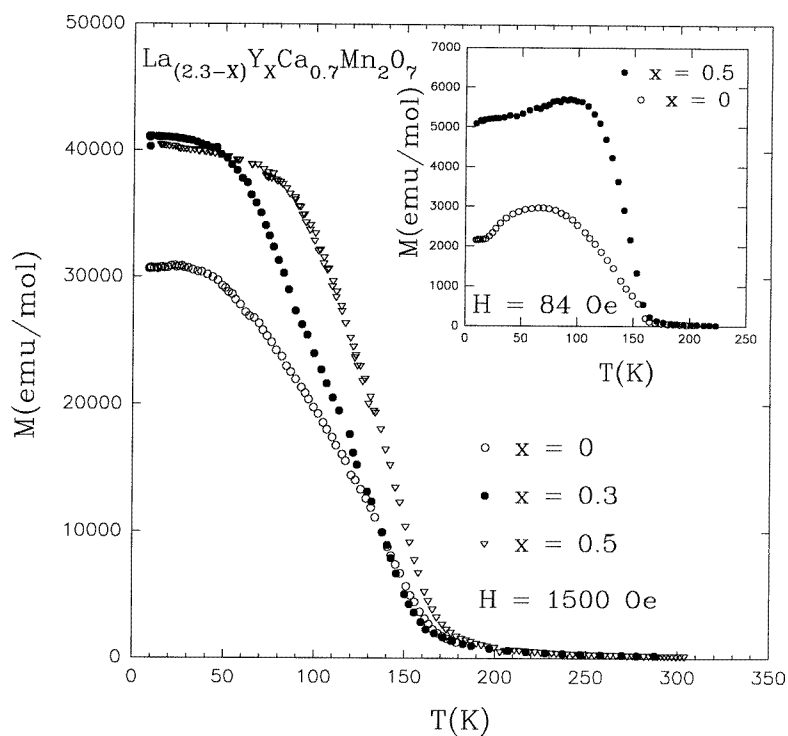


Figure 3. (a) The resistivity (ρ) of $\text{La}_{2.3-x}\text{Y}_x\text{Ca}_{0.7}\text{Mn}_2\text{O}_7$ for $x = 0, 0.3, 0.5$ as a function of temperature. (b) The MR as a function of field for $\text{La}_{1.8}\text{Y}_{0.5}\text{Ca}_{0.7}\text{Mn}_2\text{O}_7$ at $T = 4.2$ K, 60 K and 100 K.

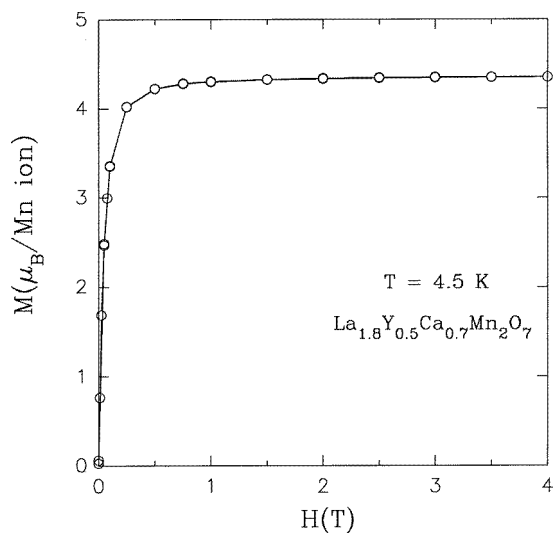
crystal structure becomes monoclinic. For $x = 0.3$ the lattice constants are $a = 3.881 \text{ \AA}$, $b = 19.285 \text{ \AA}$, $c = 4.003 \text{ \AA}$ and $\beta = 93.16^\circ$ while for $x = 0$ the lattice parameters are $a = 3.890 \text{ \AA}$, $b = 19.336 \text{ \AA}$, $c = 4.008 \text{ \AA}$ and $\beta = 93.40^\circ$. No impurity phase was detected from the XRD. It appears that the tetragonal structure is obtained when the average ionic radius at the rare-earth/alkaline-earth-metal site is same as that of $\text{La}_{1.5}\text{Ca}_{1.5}\text{Mn}_2\text{O}_7$, which has a well known tetragonal structure [3]. In this structure type the Mn–O–Mn bonds are separated along the c -axis by R(Ca)O layers. This causes the double-exchange mechanism to be stronger in the a – b plane than out of the plane, which makes the system a quasi-two-dimensional one. This has interesting effects on the electronic and magnetic properties of the material. Figure 2 shows a SEM photograph of the sample with $x = 0.5$ showing the grain structure with an average grain size of $3 \mu\text{m}$.

The resistivity ρ as a function of temperature for $\text{La}_{2.3-x}\text{Y}_x\text{Ca}_{0.7}\text{Mn}_2\text{O}_7$ ($x = 0, 0.3, 0.5$) and the MR as a function of field (up to 3.8 T) for $x = 0.5$ at various temperatures up to 100 K are shown in figures 3(a) and 3(b) respectively. The resistivity as a function of temperature (R – T) shows a peak at (T_p) 140 K for $x = 0.5$ and at 107 K for $x = 0.3$. We do not observe any metallicity for the sample with $x = 0$ though there is a slight rounding off in the R – T curve at low temperature. The residual resistance of the sample increases by almost seven orders of magnitude with change of composition from $x = 0.5$ to $x = 0$. This is in sharp contrast with the perovskite manganites, for which doping with a smaller rare-earth such as yttrium at the cation site decreases the metallicity of the sample [6]. The way the cation size affects the metallicity of the sample depends on the way in which the Mn–O–Mn bond angle changes with change in the ionic size. In the case of perovskite manganites with substitution of a small rare earth, the bond angle deviates from the ideal 180° , which in turn reduces the hopping integral t_{ij} of the e_g electrons for hopping between two neighbouring sites. It is not yet very well known how the Mn–O–Mn bond angle gets modified in the case of layered perovskite structure, where we have two types of Mn–O–Mn bond, one between two manganese ions between the bilayers and the other between two manganese ions in the same layer. However, we observe that the most highly metallic behaviour is obtained when the system goes into the tetragonal phase. The behaviour above the peak temperature is semiconducting and it is metallic below. We observe that the material with $x = 0.5$ has a MR of 60% at 4.2 K and of 93.8% at 100 K. Figure 4(a) depicts the zero-field-cooled magnetization plots measured in applied fields of 1500 Oe and 84 Oe (inset) respectively. Each of the samples has a magnetic transition temperature (T_c) in the range 160 K to 170 K, though the metallicity is completely suppressed for the composition with $x = 0$. The magnetization in Bohr magnetons per manganese ion as a function of field up to 4 T at 4.5 K for $\text{La}_{1.8}\text{Y}_{0.5}\text{Ca}_{0.7}\text{Mn}_2\text{O}_7$ is shown in figure 4(b). The saturation value $4.33 \mu_B$ is close to the value deduced from the formula for this $\text{Mn}^{2+}/\text{Mn}^{3+}$ ratio ($4.15 \mu_B$). The apparent lack of correlation between T_c and the metal–insulator transition temperature had been observed earlier for these layered perovskite compounds [3]. Asano *et al* have suggested that there are two different types of ferromagnetic coupling, possibly arising from the anisotropic double-exchange interaction [3, 7]. This might give rise to the large deviation between T_c and T_p .

Figure 5 shows the specific heat (C) as a function of temperature (T) for $x = 0, 0.3$ and 0.5 . The C versus T curve was fitted to an expression of the type $C = \gamma T + \beta T^3$ over the temperature range 2.5 K to 10 K. The values of β and γ were calculated from the slope and the intercept of the fitted C/T versus T^2 curve at $T \rightarrow 0$ respectively (inset). The Debye temperatures (θ_D), calculated from β , were found to be 329.5 K for $x = 0$, 365.9 K for $x = 0.3$ and 379.9 K for $x = 0.5$. The smaller value of θ_D for smaller x is consistent with the fact that compositions with smaller x have larger average atomic



(a)



(b)

Figure 4. (a) The magnetization (M) of $\text{La}_{2.3-x}\text{Y}_x\text{Ca}_{0.7}\text{Mn}_2\text{O}_7$ with $x = 0, 0.3, 0.5$ as a function of temperature measured at 1500 Oe (inset: the same, but measured at 84 Oe). (b) The magnetization versus the field for the sample $\text{La}_{1.8}\text{Y}_{0.5}\text{Ca}_{0.7}\text{Mn}_2\text{O}_7$ at 4.5 K up to 4 T.

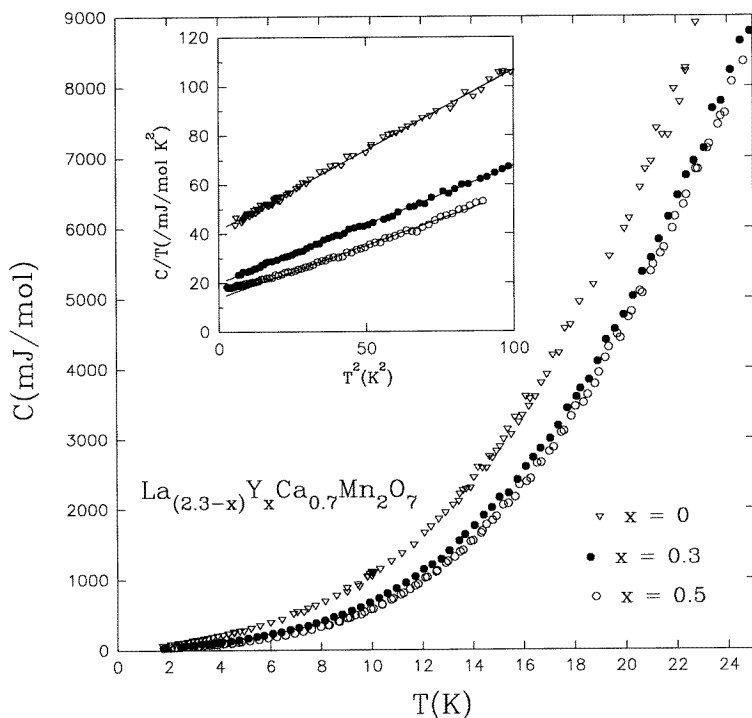


Figure 5. The temperature variation of the specific heat (C) of $\text{La}_{2.3-x}\text{Y}_x\text{Ca}_{0.7}\text{Mn}_2\text{O}_7$, for $x = 0, 0.3, 0.5$, up to 24 K (inset: C/T versus T^2 , showing linear behaviour up to 10 K).

mass at the rare-earth/alkaline-earth-metal site. The value of γ is $14.0 \text{ mJ mol K}^{-2}$ for $x = 0.5$, $20.0 \text{ mJ mol K}^{-2}$ for $x = 0.3$ and $41.5 \text{ mJ mol K}^{-2}$ for $x = 0$. The γ -values observed here are much larger than those observed for ABO_3 -type manganites which range from $4.4 \text{ mJ mol K}^{-2}$ to $6.1 \text{ mJ mol K}^{-2}$ for $\text{La}_{0.67}\text{Ba}_{0.33}\text{MnO}_3$ and $7.8 \text{ mJ mol K}^{-2}$ for $\text{La}_{0.8}\text{Ca}_{0.2}\text{MnO}_3$ [8, 9]. We believe that the two-dimensional character of the system can play an important role in the enhancement of the density of states (DOS) at the Fermi level, which might be responsible for the large value of γ observed for our compounds. This point is elaborated on in the next paragraph. There is, however, an apparent anomaly for the composition with $x = 0$ where γ , which is normally associated with the electronic contribution to the specific heat, is large though the material does not show metallicity down to 15 K. This is possibly due to magnetic phase separation in the system and is explained later.

In the perovskite manganites the fivefold-degenerate d orbital of the manganese ion splits into a threefold-degenerate t_{2g} orbital and a twofold-degenerate e_g orbital in the oxygen octahedra due to the crystal field [9]. In addition, distortion of the oxygen octahedra can split the twofold-degenerate e_g level. In the hole-doped samples the electrons in the e_g orbital get delocalized through Zener double exchange via an effective transfer integral t giving rise to conductivity and ferromagnetism. In a scenario where we have strong in-plane versus out-of-plane anisotropy we have $t_x = t_y \gg t_z$. The monoclinic distortion of the unit cell will introduce an additional reduction in the symmetry, namely $t_x \neq t_y$. In our case the manganese ions are in $\text{Mn}^{2+}/\text{Mn}^{3+}$ states with an e_g band which is slightly ($\sim 7.5\%$) more than half-filled. To understand qualitatively the effect of two dimensionality

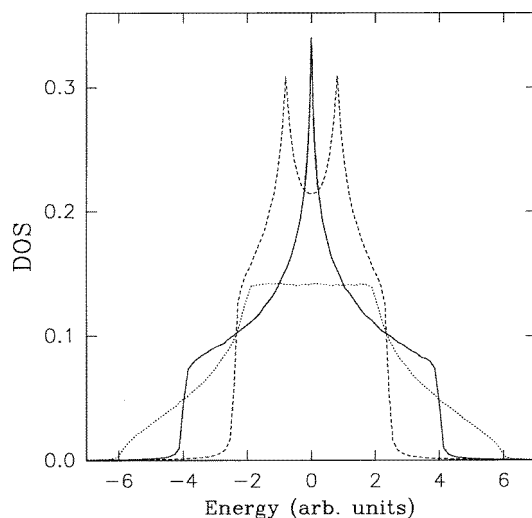


Figure 6. The DOS in 2D and 3D electronic systems neglecting the Coulomb interaction. The Fermi energy (E_F) and the DOS at the Fermi level ($N(E_F)$) for 65% filling of the band are: ($\cdots\cdots$) for 3D with $t_x = t_y = t_z = 1$, $E_F = 0.9913$ and $N(E_F) = 0.1405$ (—); for 2D with $t_x = t_y = 1, t_z = 0$, $E_F = 0.6313$ and $N(E_F) = 0.1631$; (- - -) for 2D with $t_x = 0.8, t_y = 0.4, t_z = 0$, $E_F = 0.559$ and $N(E_F) = 0.244$. The area under each is normalized to one.

on the DOS we have calculated the tight-binding DOS for two-dimensional (2D) and three-dimensional (3D) electronic systems neglecting the Coulombic repulsion between electrons and assuming certain parameter values just to illustrate the point made below. The result is shown in figure 6. It is observed that the DOS is greatly enhanced in the 2D case (where $t_x = t_y = t \gg t_z$) compared to that in the 3D case (where $t_x = t_y = t_z = t$) near half-filling of the band. The 2D DOS for $t_x \neq t_y$ is also shown in figure 6. We see that the splitting of the Van Hove singularity at half-filling of the band in two-dimensional systems can greatly enhance the DOS in the monoclinic structure for certain fillings of the band. This is likely to be the reason for the large increase of the DOS for $x = 0.3$ compared to the case for $x = 0.5$.

The apparent anomaly in γ for the composition with $x = 0$ is possibly due to magnetic phase separation in the system. Neutron diffraction studies of manganite samples have long shown that many of the hole-doped manganites become mixtures of ferromagnetic and antiferromagnetic (or canted antiferromagnetic) phases [10, 11]. We observe here that the magnetization at low temperatures (figure 4) is much smaller in the sample with $x = 0$ than for the samples with $x = 0.3$ and 0.5 both at 1500 Oe and at 85 Oe. Thus possibly the sample with $x = 0$ segregates into a mixture of ferromagnetic and antiferromagnetic phases with unconnected ferromagnetic clusters embedded in an antiferromagnetic matrix. In this situation the bulk heat capacity of the sample would include a large electronic contribution to the heat capacity associated with the ferromagnetic clusters which are metallic, but the electrical behaviour of the sample would be insulating due to the lack of a percolating conducting path. Battle *et al* [12] have recently observed from neutron diffraction studies that the compounds $\text{Sr}_{2-x}\text{Nd}_{1+x}\text{Mn}_2\text{O}_7$ are naturally biphasic with two very closely related phases, of which only one shows long-range ferromagnetic ordering. It is not clear whether a similar situation occurs for the present compound. In this context it might be noted that

from neutron diffraction studies Perring *et al* [13] had observed that the paramagnetic phase $\text{La}_{1.2}\text{Sr}_{1.8}\text{Mn}_2\text{O}_7$ consists of long-lived antiferromagnetic clusters coexisting with ferromagnetic critical fluctuations.

In summary, we have successfully synthesized the electron-doped layered manganites $\text{La}_{2.3-x}\text{Y}_x\text{Ca}_{0.7}\text{Mn}_2\text{O}_7$, $x = 0, 0.3, 0.5$, showing ferromagnetism and a metal–insulator transition for $x = 0.3$ and 0.5 . The materials display interesting behaviour in their magnetic transport and electronic properties. It would be interesting to study the electron-doped phase in detail, since the manganese e_g band which is responsible for the metallicity and ferromagnetism is symmetric with respect to half-filling of the band in the parent material (with all ions in the Mn^{3+} state). We believe that the apparent lack of correlation between T_c and the metal–insulator transition and also the enhancement of γ with increasing monoclinic distortion can be understood by considering the effect of anisotropic double exchange in the Mn–O–Mn network.

One of the authors (PR) would like to thank Srikantha Sil for pointing out the role of two dimensionality in the DOS in these systems. The authors would also like to thank S B Roy for his help regarding SQUID measurements.

References

- [1] Morimoto Y, Asamitsu A, Kuwahara H and Tokura Y 1996 *Nature* **380** 141
- [2] Seshadri R, Martin C, Hervieu M, Raveau B and Rao C N R 1997 *Chem. Mater.* **9** 270
- [3] Asano H, Hayakawa J and Matsui M 1996 *Appl. Phys. Lett.* **68** 3638
- [4] Battle P D, Blundell S J, Green M A, Hayes W, Honold M, Klehe A K, Laskey N S, Millburn J E, Murphy L, Rosseinsky M J, Samarin N A, Singleton J, Sluchanko N E, Sullivan S P and Vente J F 1996 *J. Phys.: Condens. Matter* **8** L427
- [5] Zener C 1951 *Phys. Rev.* **82** 403
- [6] Fontcuberta J, Martinez B, Seffar A, Pinol S, Garcia-Munoz J L and Obradors X 1996 *Phys. Rev. Lett.* **76** 1122
- [7] Asano H, Hayakawa J and Matsui M 1997 *Appl. Phys. Lett.* **70** 2303
- [8] Hamilton J J, Keatley E L, Ju H L, Raychaudhuri A K, Smolyaninova V N and Greene R L 1996 *Phys. Rev. B* **54** 14926
- [9] Coey J M D, Viret M, Ranno L and Ounadjela K 1995 *Phys. Rev. Lett.* **75** 3910
- [10] Wollan E O and Koehler W C 1955 *Phys. Rev.* **100** 545
For a recent review regarding this aspect of manganite materials, see Nagaev E L 1996 *Sov. Phys.–Usp.* **39** 781 and references cited therein
- [11] Jirak Z, Hejtmanek J, Pollert E, Marysko M, Dlouha M and Vratislav S 1997 *J. Appl. Phys.* **81** 5790
- [12] Battle P D, Green M A, Laskey N S, Millburn J E, Radaelli P G, Rosseinsky M J, Sullivan S P and Vente J F 1996 *Phys. Rev. B* **54** 15967
- [13] Perring T G, Aeppli G, Morimoto Y and Tokura Y 1997 *Phys. Rev. Lett.* **78** 3198